Journal of Chromatography, 351 (1986) 17–29
Elsevier Science Publishers B.V., Amsterdam — Printed in The Netherlands

CHROM. 18 179

EXPERIMENTAL AND THEORETICAL DYNAMICS OF ISOELECTRIC FOCUSING

ELUCIDATION OF A GENERAL SEPARATION MECHANISM

W. THORMANN, R. A. MOSHER* and M. BIER
Center for Separation Science, University of Arizona, Tucson, AZ 85721 (U.S.A.)
(First received June 24th, 1985; revised manuscript received September 16th, 1985)

SUMMARY

The transient states in isoelectric focusing were monitored using a potential gradient array detector. Electric field profiles are presented which show the formation of transient moving boundaries, as well as the approach of the steady state distribution, during the focusing of two and three component systems. The experimental results are completely consistent with corresponding computer simulation data. The focusing process is comprised of two sequential phases, a relatively rapid separation phase and a much slower stabilizing phase. A phenomenological separation mechanism is presented for the two and three component systems, based on distinct, transient moving boundaries, which describes the first phase. This mechanism is discussed with respect to *n* component idealized systems. The second phase provides insight into a primary cause of pH gradient instability. It was found that the time necessary for the adjustment to the steady state, the second phase, can be as much as twenty times longer than the time needed for the separation of the constituents.

INTRODUCTION

A knowledge of the dynamics in isoelectric focusing (IEF) is essential for the characterization of this electrophoretic mode. Various procedures for the determination of transient states have been developed. Repetitive scanning of the focusing column with an optical detector[1], a pH sensor[2] or a radiometric detector[2] has been employed. The measuring of schlieren patterns or shadowgrams[3], the visual inspection or photographic registration of fluorescing carrier and/or test components as well as of colored proteins represent alternate methods. Another approach consists of segmentation of gels or paper strips after various times of current flow, followed by pH, conductance, absorbance, radioactivity or other measurements, such as bioassays, on the segments[4]. Comparable procedures include the freezing and segmentation of a plastic tube containing the medium to be tested[5] and the evaluation of fractions collected from density stabilized columns[6]. None of these methodologies provide complete insight into the evolution of the entire IEF pattern, but do permit monitoring the kinetics of specific constituents.

0021-9673/86/$03.50

The electric field is the most general physical property in electrophoresis. Its distribution along an isoelectric focusing column is important for both theoretical and practical purposes. Without accurate measurement of the local potential gradient it is particularly difficult to give a physicochemical description of the separation mechanism or of a focused zone. The local electric field strength further determines the migration rate of components and the generation of heat. The potential gradient across IEF gel slabs is commonly measured by inserting one or two electrodes into evenly spaced holes in the top of a slab apparatus[7], with sliding contacts or by conductivity measurements on segmental fractions referred to above[4–6]. Jackiw *et al.*[8] constructed a device for measuring the voltage gradient along tube gels. Their detector consists of 11 platinum sensors sealed into the wall of a Pyrex tube (6 mm I.D.) at 1-cm intervals.

We incorporated an array detector as one wall of the separation trough, which enables us to make almost simultaneous measurements of the potential gradient at 100 (or 255) equidistant positions along a 10-cm column[9]. The construction of the apparatus is based on the principle described by Thormann *et al.*[10] for the detection of transient and steady state zone structures in electrophoresis. Monitoring the electric field with this array detector permits following the dynamics in a continuous fashion, under full computer control. The apparatus allows focusing in free solution. Resolution is far better than that of Jackiw *et al.*[8], thus permitting a detailed monitoring of the focusing process. Data showing the focusing dynamics of systems comprising two and three buffer components are given which illustrate the mechanism of separation.

There have been many theoretical treatments of the focusing of components in an equilibrium gradient[11–22]. Most of these have utilized simplified models. Descriptions of the equilibrium distribution of sample components[12–14] and of the resolution in IEF[15,16] are based on several restrictive assumptions, including constant conductivity and linear pH gradients. Steady state concentration, pH and conductivity profiles have been calculated with simplified mathematical models[17,18] and by sophisticated computational analysis[19]. Theoretical discussions of transient states are confined to systems where the focusing of an ampholyte is described in a preestablished, linear pH gradient[20]. Computer modeling is the only methodology at hand for the prediction of concentration, pH and conductivity profiles as functions of time[21,22]. The general model of Bier *et al.*[22] predicts the salient features of all the classically recognized methods in electrophoresis, including IEF. It is based upon equations describing the component's chemical equilibria, electroneutrality as well as conservation of mass and charge, and computes the net mass transport of each component due to electromigration and diffusion. This model, in contrast to that of Svendsen *et al.*[21], is not restricted to electromigration only and incorporates the proper boundary conditions for IEF. In this paper computer simulation data are employed, in conjunction with experimental data, to describe the mechanism of focusing of two and three component mixtures. This mechanism is then generalized to specialized systems to elucidate a general focusing mechanism of n components.

MATERIALS AND METHODS

Potential gradient measurements

Our apparatus comprises a rectangular separation trough (about 0.4 × 1 mm)

with an ordered array of 100 electrodes over the total length of 10 cm[9]. Gold electrodes are produced by silk screening of formulated metallo-organics on a Pyrex glass plate, followed by heat decomposition of the organic matrix. The electrodes have a width of about 0.025 cm, a height of about 0.2 μm and are 0.076 cm apart. The rectangular focusing trough is defined by a silicone rubber gasket between the glass plate and a block of plexiglass. This block contains the electrode assemblies. The electrode array is enlarged at the outer edge of the detector plate to allow mechanical scanning[9]. The potential gradient between adjacent electrodes is monitored and the data are processed and stored in the computer. A complete scan consists of 99 data points and requires 14 min in the present configuration.

All presented experiments were performed in free solution and at ambient temperature. The current was a constant 10 μA unless otherwise indicated. Electrode assemblies included dialysis membranes for the isolation of the focusing column from the electrode compartments. The anolyte and catholyte solutions were 0.1 *M* phosphoric acid and 0.1 *M* sodium hydroxide, respectively. The solution with carrier components was uniformly distributed throughout the column before application of the constant driving current. Analytical grade chemicals were used as available.

Computer simulations

Our computer model is one dimensional and assumes the absence of convective flows or thermal gradients. No *ad hoc* stipulations are made concerning pH or voltage gradients, rather these profiles are computed as a part of the solution. The focusing column is overlaid with a set of grid points for discretization of the spatial derivatives. Central differences are used wherever possible, with forward and backward differences used at the boundaries. The resulting ordinary differential equations with time as the independent variable are integrated using software developed on the basis of DARE-P language[23,24]. The inputs required to perform a simulation include the dissociation constants of the compounds, mobility coefficients of the positive, negative and neutral species, initial concentration of the components in the column, cross sectional area and length of the column and the current. The amount of electrophoresis time is also specified. The values used for the presented example are summarized in Table I. The boundary conditions are given by the assumption that the current across the ends of the column is carried by hydrogen and hydroxyl ions only[22]. The outputs from a simulation are the concentration of each component at each grid point across the column, and the pH and conductivity profiles. The maximum relative local truncation error for these simulations, as computed by the order difference method, is $1.0 \cdot 10^{-4}$.

RESULTS AND DISCUSSION

Experimental investigation

The focusing of three different 3 component systems and one 2 component system has been monitored. The data obtained from all systems are consistent with a general mechanism of isoelectric focusing which is represented schematically in Fig. 1. The physical properties of the three components were chosen such that constituent A is the most basic, C the most acidic and B has an intermediate isoelectric point. Focusing is divided into two phases, a separation phase and a stabilizing phase. The

TABLE I

CONDITIONS FOR COMPUTER SIMULATION

General values			
Column length	1 cm		
Segmentation	100 segments/cm		
Current density	0.001 A/cm^2		
pK_a and mobility values			
Component	*pK_{a_1}*	*pK_{a_2}*	*Mobility $\times 10^4$ [cm^2/Vs]**
Glutamic acid	2.16	4.29	2.97
Histidine	6.02	9.17	2.85
Arginine	9.04	12.48	2.26
H_3O^+			36.27
OH^-			19.87

* It was assumed that all species of a component have equal mobility coefficients. Note that this is not required by our model.

separation phase comprises two clearly distinguishable classes of transient stages. The initial stage (a) and stage (c) represent distinct time points whereas the transient stages (b) and (d) are characteristic time intervals during which five-zone structures are present. Fig. 1e shows complete separation of the 3 constituents and marks the start of the stabilizing phase.

Fig. 1a depicts the initial state prior to voltage application with all components evenly distributed. Transient stage (b) is characterized by the formation of two transient moving boundaries from each electrode. α_1 is the boundary between the zone of pure component A at the cathode, and a mixed zone composed of A and the intermediate component B. The boundary α_2 is the demarcation between a zone of pure component C at the anode and a mixed zone of B and C. The more rapidly migrating β boundaries separate the initial mixture and the transient mixed zones A–B and B–C. They represent the trailing boundaries of the faster components; β_2 for A on the anodic side and β_1 for C on the cathodic side. This is indicated by the letters below the vectors. Both the transient stages (b) and (d) are five-zone structures whereas the time point (c) comprises four zones only. When the faster β boundaries meet, the pure zone of constituent B starts to evolve. This corresponds to the time point depicted in Fig. 1c. Two new boundaries appear, γ_1 and γ_2, which migrate in opposite directions. These are the evolving fronts of the pure zone of component B [transient stage (d)]. Each merges with a corresponding α boundary approaching from the column end to produce the boundaries δ_1 and δ_2. This configuration, presented as Fig. 1e, is the end of the separation phase. δ_1 and δ_2 slowly migrate toward their proximal electrodes. The approach to the steady state distribution (Fig. 1f) denotes the end of the stabilizing phase. The separation scheme presented assumes that the two δ boundaries are formed simultaneously. This is, of course, a somewhat idealized situation. In reality, transient stage (d) is first reduced to a four-zone struc-

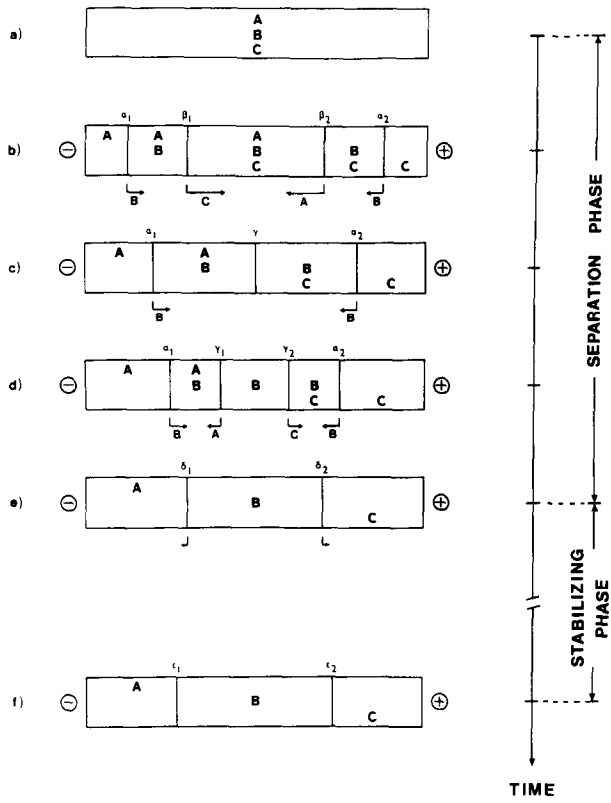

Fig. 1. Idealized schematic presentation of the focusing stages with three buffer components. Component A is the most basic, C the most acidic and B has an intermediate isoelectric point. The boundaries between zones are depicted by vertical solid lines and denoted by greek letters. The vectors indicate the direction and the relative velocity of the migrating boundaries. The letters below the vectors denote the component responsible for the boundary. Stages (a) to (e) depict the separation phase. Between stages (e) and (f) the system stabilizes and attains steady state. To simplify matters it is assumed that the two δ boundaries are formed simultaneously and that the three components have similar concentration in the initial mixture.

ture with one δ boundary before the three-zone configuration of Fig. 1e is established. It is also assumed that the three components have similar concentration in the initial mixture.

Fig. 2 shows the dynamics of the electric field during the focusing of a mixture of 3 amino acids, arginine, histidine and glutamic acid, which correspond to components A, B and C respectively, of Fig. 1. The boundaries α_1, β_1 and α_2 are present by scan 3. The field change across the β_2 boundary was insufficient to be detected in this system. The spike in the center of scan 8 indicates the onset of transient stage (d), the beginning of the evolution of the pure histidine zone. The γ boundaries are fully established by scan 9 and the two δ transitions are detected by scan 11. Scan 10 illustrates that the two δ boundaries are not formed simultaneously, the δ_2 transition being established first. Each experimental electric field profile in this and other figures has been corrected for irregularities in the cross sectional area of the column[25].

The transient behavior of the voltage gradient during the focusing of a mixture

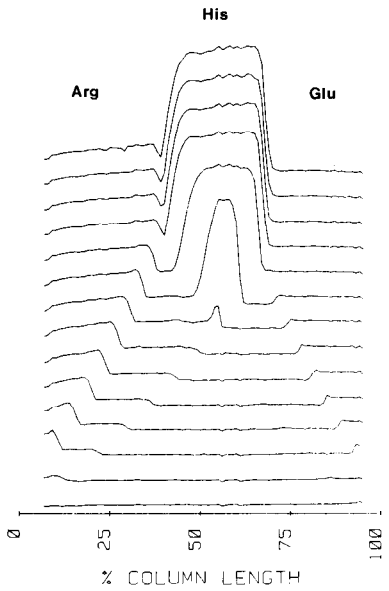

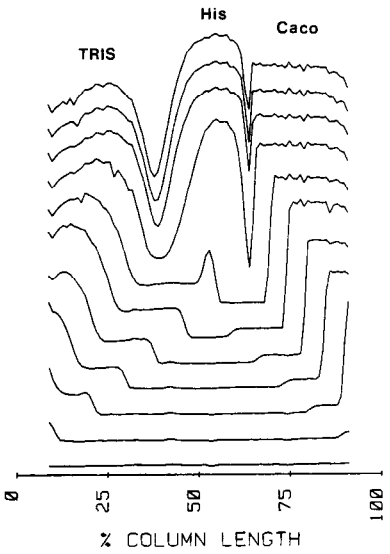

Fig. 2. Dynamics of the potential gradient monitored during the focusing of a mixture of arginine (Arg), histidine (His) and glutamic acid (Glu). Initial concentrations were 10 mM each. The pH of the mixture was 7.47 and the conductivity 0.469 mS/cm. The bottom scan is the uniform profile obtained just after application of the current. The scan interval was 21 min with each successive scan offset from the previous one by 0.5 V. The final focusing voltage across the whole cell was about 150 V. The anode is to the right.

Fig. 3. Dynamics of the electric field monitored during the focusing of Tris, histidine (His) and cacodylic acid (Caco). The initial concentrations were 8.27, 7.05 and 8.76 mM respectively. The pH of the mixture was 7.36 and the conductivity 0.438 mS/cm. The final focusing voltage was about 300 V. Other conditions as in Fig. 2.

of the base Tris [tris(hydroxymethyl)aminomethane], the amino acid histidine and cacodylic acid is depicted in Fig. 3. These correspond to components A, B and C respectively, of Fig. 1. All four boundaries, the two α and the two β, of the separation phase are present by scan 3. The evolution of the pure histidine zone has begun by scan 7. The δ boundary between Tris and histidine is much more broad than that between histidine and cacodylic acid. This is consistent with the computer predicted profile reported in ref. 22. The two presented systems clearly reveal that the more rapidly migrating β boundaries are characterized by a substantially smaller field change than are α boundaries. This is because the α boundaries border zones of pure compounds which are less conductive. The γ and δ boundaries represent substantial field changes.

Two amino acids and a dipeptide comprise the mixture used to obtain the data in Fig. 4. Arginine and *p*-aminobenzoic acid correspond to components A and C respectively, and L-lysyl-1-aspartic acid represents the intermediate constituent B, of Fig. 1. Both α and β boundaries are visible by scan 2. The beginning of transient stage (d) is marked by a substantial increase in the voltage gradient in the center of the column. The detected signal even becomes too large for the data aquisition system as shown by the recorder going off scale in scan 7 of Fig. 4a. The pure zone of the dipeptide has a very low conductivity. To obtain the complete profile of Fig. 4b, the

current was decreased from 10 μA to 2.5 μA. The α_2 boundary in this system is unusual because the electric field increases across the boundary in the direction of migration, whereas all other experimentally detected boundaries exhibit a field decrease in the direction of migration. A field decrease across an electrophoretic boundary in the direction of migration produces a steady state shape[26]. All detected boundaries which fit this criterion appear to exhibit a steady state. It is difficult to determine from the data however, whether the α_2 boundary of Fig. 4a is becoming broader as it migrates.

The registration of the focusing current under constant voltage is an alternate way of characterizing the focusing process. Fig. 5 presents the temporal behavior of the current for the system of Fig. 4. The applied voltage was a constant 100 V. The current decreases substantially as focusing progresses. The distinct inflection point in this graph (shown by the arrow) was found to mark the time point of transient stage (c) of Fig. 1, *i.e.* the start of the evolution of the pure middle zone with high resistance [transient stage (d)]. This point is also present in the current-time plots of the systems shown in Figs. 2 and 3 (data not shown) although it is less pronounced because of the higher relative conductivity of their central zones.

Fig. 6 depicts the experimentally determined transient and steady state electric field profiles during the focusing of glutamic acid and histidine. This experiment

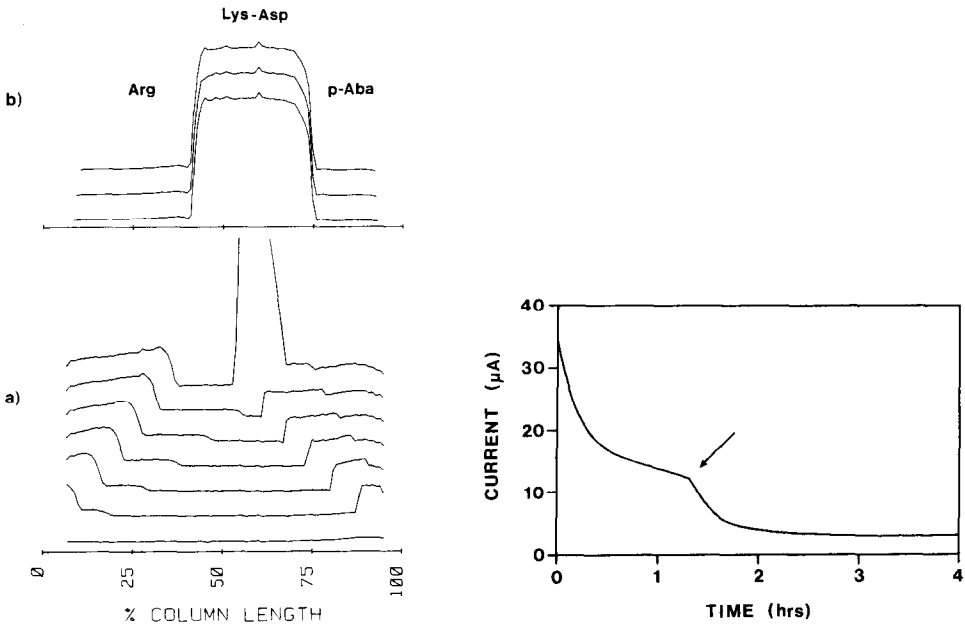

Fig. 4. Dynamics of the potential gradient monitored during the focusing of arginine (Arg), lysyl–aspartic acid (Lys–Asp) and *p*-aminobenzoic acid (*p*-Aba). Initial concentrations were 8, 10 and 6 m*M* respectively. The pH of the mixture was 7.29 and the conductivity 0.406 mS/cm. Scans 1–7 were monitored with a constant current of 10 μA (a) and scans 13–15 were registered at a constant current of 2.5 μA (b). The focusing voltage at this stage was about 400 V. Other conditions as in Fig. 2.

Fig. 5. Variation of current during focusing under a constant 100 V of the system shown in Fig. 4. The arrow indicates the time point of transient state (c) of Fig. 1.

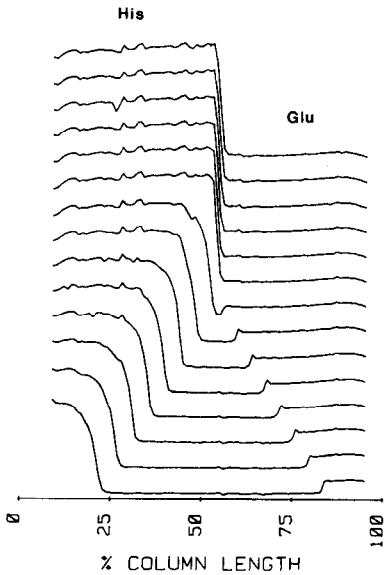

Fig. 6. Dynamics of the potential gradient monitored during the focusing of histidine (His) and glutamic acid (Glu). Initial concentrations were 15 m*M* each. The pH of the mixture was 5.23 and the conductivity 0.645 mS/cm. The final focusing voltage across the whole cell was about 180 V. The anode is to the right. Other conditions as in Fig. 2.

clearly illustrates the formation of two transient moving boundaries; one arising from the anode, the other from the cathodic column end. They are interfaces between the evolving zones of pure amino acids and the initial mixture. The boundary arising from the cathodic end is the trailing boundary of glutamic acid and corresponds to α_1 of Fig. 1. The trailing boundary of histidine originates at the anode and is equivalent to α_2 of Fig. 1. Both are migrating toward the center of the column, where a stationary boundary is formed. The two migrating boundaries have a steady state shape across which the electric field increases opposite to the direction of migration. They also represent pH gradients.

Theoretical investigation

Fig. 7 depicts the computer predicted concentration, pH and conductivity profiles for the system of Fig. 2. The simulation conditions are summarized in Table I. The conductivity profiles are nicely consistent with the experimentally detected evolution of the electric field. Not only the number of transient boundaries representing electric field changes matches those experimentally monitored, but also their relative velocities, such as the earlier establishment of boundary δ_2 compared to δ_1, agree nicely. The corresponding concentration profiles illustrate the composition of the zones defined by the transient boundaries. The excellent correlation between the theoretical predictions and experimental data confirm the mechanism of IEF presented schematically in Fig. 1. Other simulations with three buffer components[22,23] and the predictions for two component systems (not displayed) have produced similar results. Although the array detector provides outstanding resolution, it is not capable of discerning all of the fine structure predicted within a boundary. The conductivity

spike present in the histidine-arginine boundary in Fig. 7 is mirrored in the experimental data of Fig. 2, but the corresponding spike in the histidine–glutamic acid boundary was not monitored. The experimental current density was about twice that used for the computer simulation, and the spike in the latter boundary is apparently either too sharp to be observed or even absent due to convective disturbances caused by the temperature gradient across the boundary. The effects of temperature gradients are not included in our mathematical model. The relative conductivities of the focused zones of pure components are different in the experimental and simulation data. This is due to the actual mobility of histidine being different from the value used in the simulation and due to the neglection of temperature gradients.

The boundaries present after full separation of the three components (*cf.* scans 11–14 in Fig. 2) were found to slowly migrate towards either column end. This effect is best illustrated by Fig. 8 in which the scan interval was increased to about one hour. The observation time of approximately 15 h is much longer than needed for complete separation of the three amino acids. Fig. 9 displays the potential gradient distribution of the same system after 4 h (solid line) and a scan taken after 18 h of current flow (broken line). The arginine–histidine boundary in the cathodic half of the column was found to migrate about twice as fast as the anodic boundary and the two profiles exhibit a field increase in the middle zone as electrophoresis progresses. Both effects are in good agreement with our simulation analysis. The computed profiles presented in Fig. 7 illustrate a similar displacement of the two final boundaries (δ boundaries of Fig. 1) between 25 and 150 min. The histidine–glutamic acid boundary is predicted to migrate a bit away from the anode between 150 and 400 min of current flow. This and related effects may be attributable to the concentration slope of the histidine zone at 150 min which must revert to being flat. Further data after

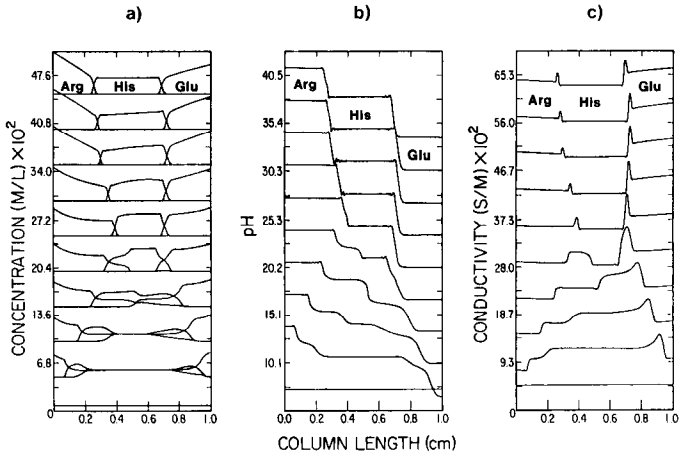

Fig. 7. Computer predicted concentration (a), pH (b) and conductivity (c) profiles for the simulated mixture of arginine (Arg), histidine (His) and glutamic acid (Glu). The time points plotted, from bottom to top, are 0, 5, 10, 15, 20, 25, 50, 100, 150 and 400 min of current flow. Each successive set of concentration profiles is offset from the previous set by 50 m*M*. The offsets for the conductivity and pH profiles are 0.07 S/m and 3.4 pH units respectively. Initial concentrations were 10 m*M* each. See Table I for additional data. The damped sinusoidal oscillations are numerical in nature and do not represent true fluctuations in the concentrations. The anode is to the right.

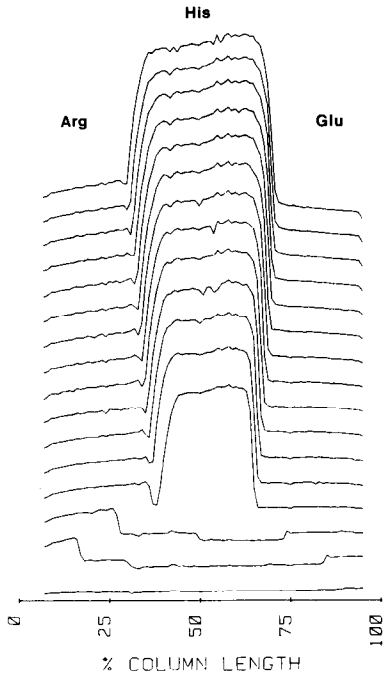

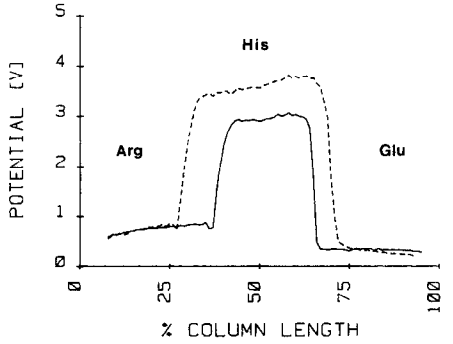

Fig. 8. Dynamics of the electric field during the extended focusing of arginine (Arg), histidine (His) and glutamic acid (Glu), the same system depicted in Fig. 2. The scan interval was 1 h. All other conditions as in Fig. 2.

Fig. 9. A comparison of the potential profiles detected after 4 h (solid line), and after 18 h (broken line) of focusing of the system presented in Figs. 2 and 8.

500, 600, 700 and 800 min and the prediction of our steady state IEF program[19] were found to be equivalent to the profiles obtained after 400 min of current flow. With the 2 component system presented in Fig. 6 a small displacement of the final boundary towards the anode was both experimentally observed and theoretically computer predicted. This indicates the existence of two phases during the focusing of two and three components; first the constituents separate according to the principle shown for three components in Fig. 1a–e, which we call the separation phase. This is followed by a stabilizing phase which results in the attainment of the true steady state. The mechanistic description presented in the separation phase is in complete accord with the concepts of Svendsen and Schafer-Nielsen[21].

The drifting boundaries in the stabilizing phase are a manifestation of pH gradient instability, a phenomenon which has been thoroughly studied (for a review see ref. 4, pp. 299–303). The data presented provide an explanation for the observation of the formation of a pH plateau in the neutral region with a decrease in the number of stainable ampholyte species there and an increase in the stainable ampholyte species at the ends of the gradient[28]. The details of the mechanism causing this instability are currently under investigation[29]. Our simulation data indicate that the stabilizing phase for the system depicted in Figs. 2, 7 and 8 is roughly fifteen times as long as the separation phase. It is harder to determine the relative lengths

of these two phases from experimental data. This is because there are several factors which contribute to pH gradient instability. Our experiments utilized dialysis membranes to separate the focusing capillary from the electrode compartments[9]. These are not perfect boundary conditions for IEF because of the permeability of the membranes to the ampholytes and electrode solutions. The experimental systems described herein were found to degrade after about 20 h of current flow.

CONCLUSIONS

A detector array of the type utilized in these experiments is capable of providing valuable information concerning the dynamics of IEF. Both transient and steady state zone distributions can be monitored. The experimental data represent the first visualization of the moving boundaries present during the transient stages of IEF. Jackiw *et al.*[2,8] failed in this respect because of the limited resolution of their apparatus. These results and those presented in refs. 10, 22 and 27 clearly indicate that moving boundaries, at least as transient phenomena, are ubiquitous in all modes of electrophoresis.

The combination of computer modelling and appropriate experimental data provides a powerful tool for the analysis of electrophoretic systems. The excellent agreement between these approaches has allowed an unambiguous definition of the composition of the zones on either side of each transient moving boundary present in the laboratory data. This made it possible to construct a theory describing the dynamics of three component IEF systems which is applicable to systems containing ampholytes as well as weak acids and bases. In the configurations studied focusing proceeds in two phases, a relatively rapid separation phase and a much slower stabilizing phase. The latter is an adjustment to the theoretical steady state, and can be as much as twenty times as long as the former at constant current. It is present when the pH gradient encompasses regions significantly far from neutrality. This phase occurs because the zones of pure acidic and basic ampholytes do not have flat concentration profiles at the steady state[12]. After the initial, rapid condensation of these components into pure zones (separation phase), the concentration profiles slowly acquire a slope, increasing in the direction of the cathode in the case of basic ampholytes, and in the direction of the anode with acidic ampholytes. This is attributable to the inequality in the concentration of the positively and negatively charged species. The presence of hydrogen ions in a zone of pure acidic ampholyte requires, as a consequence of electroneutrality, that the concentration of the negatively charged ampholyte species is greater than that of positively charged species by an amount equal to the hydrogen ion concentration. Similar relationships apply for the basic column end with hydroxyl ions and positively charged ampholyte species respectively. Thus, even condensed zones of ampholytes at their isoelectric points have a net charge and therefore a tendency to migrate electrophoretically. The slope of the final concentration profile simply reflects the equal and opposite mass transports due to diffusion and electromigration which characterizes the IEF steady state. The stabilizing phase provides insight into one of the contributing factors to pH gradient instability. This is currently being analyzed in depth in our laboratory and will be reported in due course[29].

The mechanism by which two and three buffer components focus is clearly

defined by the amalgam of experimental and simulation data. The elucidated mechanism holds for systems comprising amino acids, small peptides and weak monovalent acids and bases. The acids and bases must be the most acidic or basic components respectively in the mixture, however, for the mechanism to apply. A system composed of glutamic acid, cacodylic acid and histidine, for example, would be unlikely to focus according to the mechanism described because of the relative acidities of the glutamic and cacodylic acids and, of course, the non amphoteric nature of cacodylic acid.

During the separation phase described for two ($n = 2$) and three ($n = 3$) components, two classes of transient stages are distinguishable if it is assumed that the two δ boundaries are formed simultaneously (Fig. 1): (i) $n - 1$ transient stages representing time intervals during which a $2n - 1$ zone structure is present; and (ii) n intermediate transient time points, the first being the initial stage (one zone configuration), the second representing the stage when the first two boundaries meet (two-zone structure for $n = 2$; four-zone structure for $n = 3$) and when $n = 3$, the third being the stage when the final three-zone configuration is formed. A transient moving boundary is attributable to a single component, as is indicated by the letters below the vectors in Fig. 1. Whenever $n > 2$, the separation phase will contain time points when two boundaries, travelling in opposite direction, meet and two new boundaries migrate away from the meeting point. That the boundaries which leave this meeting point are attributable to the same components as were the boundaries which met could lead to the erroneous impression that this is simply two boundaries crossing. In electrophoretic theory, however, boundaries are usually defined by the composition of the zones on either side. It is therefore clear from the simulation data that new boundaries form at these time points.

The focusing process of n ampholytes ($n > 3$) becomes very complex. Essentially such a system is producing distinct transient states with moving boundaries which consist of more than $n - 1$ characteristic time intervals referred to above. The focusing mechanism presented in Fig. 1 can be generalized to describe the focusing of n ampholytes, if it is assumed that these components have evenly spaced isoelectric points, nearly equivalent ionic mobilities and ΔpK_a values and have similar concentrations in the initial mixture. Such a system will produce $n - 1$ transient time intervals, each characterized by distinct $2n - 1$ zones and punctuated by stages representing points in time when boundaries meet. A total of n such time points are present which mark the disappearance of certain zones and the appearance of new zones. The first is the initial stage (one-zone configuration). The subsequent $n - 1$ time points are characterized by a stepwise decrease in their zone number from $2n - 2$ to n. This general description of the focusing process for n ampholytes was verified by computer simulation. While the mechanism applies only to restricted situations, we believe that it is a valuable aid to the understanding of IEF. It does not describe systems containing a variety of weak acids and bases, but such components are allowed to be the most acidic and the most basic constituents respectively. The summation of the number of transient stages representing time intervals and the number of time points for an idealized situation, $2n - 1$, represents the minimum theoretical number of transient states produced during the separation phase of n components.

Complex mixtures of real ampholytes, such as mixtures of synthetic carrier

ampholytes, will be unlikely to follow precisely the mechanism presented and will produce more than $2n - 1$ transient states during the separation phase. This is due to an unequal distribution of their isoelectric points, unequal net mobilities due to both unequal ionic mobilities and unequal ΔpK_a values, and differences in the initial concentrations in the mixture. However, the existence of the two phases during focusing was verified experimentally using synthetic carrier ampholyte mixtures in our capillary device[30].

ACKNOWLEDGEMENTS

The authors would like to acknowledge valuable discussions with Dr. N. B. Egen, the experimental assistance of L. Zawadsky and the careful presentation of computer generated data by J. Walker. This work was partly supported by NASA grant NSG-7333, NSF grant CPE-8311125 and by a grant from the Swiss National Science Foundation.

REFERENCES

1 N. Catsimpoolas, in P. G. Righetti (Editor), *Progress in Isoelectric Focusing and Isotachophoresis*, North Holland, Amsterdam, 1974, pp. 77–92.
2 B. A. Jackiw and A. Chrambach, *Electrophoresis*, 1 (1980) 150.
3 E. Fries, *Anal. Biochem.*, 70 (1976) 124.
4 P. G. Righetti, *Isoelectric Focusing: Theory, Methodology and Applications*, Elsevier, Amsterdam, 1983.
5 W. J. Gelsema, C. J. de Ligny and N. G. van der Veen, *J. Chromatogr.*, 173 (1979) 33.
6 S. Fredriksson, *J. Chromatogr.*, 135 (1977) 441.
7 A. Murel, S. Vilde, A. Kongas and O. Kirret, *Electrophoresis*, 5 (1984) 139.
8 B. A. Jackiw, B. E. Chidakel, A. Chrambach and R. K. Brown, *Electrophoresis*, 1 (1980) 102.
9 W. Thormann, G. Twitty, A. Tsai and M. Bier, in V. Neuhoff (Editor), *Electrophoresis '84*, Verlag Chemie, 1984, Weinheim, pp. 114–117.
10 W. Thormann, D. Arn and E. Schumacher, *Electrophoresis*, 5 (1984) 323.
11 A. Kolin, *Proc. Natl. Acad. Sci. U.S.A.*, 41 (1955) 101.
12 H. Svensson, *Acta Chem. Scand.*, 15 (1961) 325.
13 E. Schumacher, *Helv. Chim. Acta*, 40 (1957) 2322.
14 W. G. Kauman, *Classe des Sciences de l'Academie Royale de Belgique*, 43 (1957) 854.
15 J. C. Giddings and K. Dahlgren, *Sep. Sci.*, 6 (1971) 345.
16 H. Rilbe, *Ann. N.Y. Acad. Sci.*, 209 (1973) 11.
17 M. Almgren, *Chemica Scripta*, 1 (1971) 69.
18 K. Shimao, *Seibutsu Butsuri Kagaku*, 24 (1981) 59.
19 M. Bier, R. A. Mosher and O. A. Palusinski, *J. Chromatogr.*, 211 (1981) 313.
20 G. H. Weiss, N. Catsimpoolas and D. Rodbard, *Arch. Biochem. Biophys.*, 163 (1974) 106.
21 P. J. Svendsen and C. Schafer-Nielsen, in D. Stathahkos (Editor), *Electrophoresis '82*, Walter de Gruyter, Berlin, 1983, pp. 83–89.
22 M. Bier, O. A. Palusinski, R. A. Mosher and D. A. Saville, *Science*, 219 (1983) 1281.
23 G. A. Korn and J. V. Wait, *Digital Continuous System Simulation*, Prentice-Hall, Englewood Cliffs, N.J., 1978.
24 A. Graham, O. A. Palusinski, R. A. Mosher, M. Bier and D. A. Saville, *Proceedings of the 10th IMACS World Congress on System Simulation and Scientific Computations*, Vol. 4, International Association for Mathematics and Computers in Simulation, Montreal, 1982, pp. 92–94.
25 E. Schumacher, D. Arn and W. Thormann, *Electrophoresis*, 4 (1983) 390.
26 R. A. Mosher, W. Thormann and M. Bier, *J. Chromatogr.*, 320 (1985) 23.
27 W. Thormann, R. A. Mosher and M. Bier, in V. Neuhoff (Editor), *Electrophoresis '84*, Verlag Chemie, Weinheim, 1984, pp. 118–121.
28 R. Frater, *Anal. Biochem.*, 38 (1970) 536.
29 R. A. Mosher, W. Thormann and M. Bier, *J. Chromatogr.*, 351 (1986) 31–38.
30 W. Thormann, N. B. Egen, R. A. Mosher and M. Bier, *J. Biochem. Biophys. Methods.*, 11 (1985) 287.